Systems Microbiology and Biomanufacturing (2022) 2:705–715
https://doi.org/10.1007/s43393-022-00102-x

ORIGINAL ARTICLE

Multi-enzyme cascade for sustainable synthesis of L-*threo*-phenylserine by modulating aldehydes inhibition and kinetic/thermodynamic controls

Yuansong Xiu[1] · Guochao Xu[1] · Ye Ni[1]

Received: 18 March 2022 / Revised: 14 April 2022 / Accepted: 17 April 2022 / Published online: 7 May 2022

Abstract

L-Threonine transaldolase could catalyze the transaldolation of L-threonine and aldehyde to generate β-hydroxy-α-amino acids with high diastereoselectivity. A novel L-threonine transaldolase (*Pm*LTTA) was identified from *Pseudomonas* sp. through genome mining. *Pm*LTTA exhibited high activity in the synthesis of L-*threo*-phenylserine from L-threonine and benzaldehyde, with specific activity of 5.48 U mg^{-1}. However, the application of *Pm*LTTA was impeded by the low conversion ratio and variable diastereoselectivity, which were caused by the toxicity of aldehydes and kinetic/thermodynamic controls in the transaldolation reaction. To solve these issues, alcohol dehydrogenase was used to remove the by-product acetaldehyde, and then carboxylic acid reductase was introduced to alleviate the inhibition of benzaldehyde and toxicity of DMSO. Finally, a multi-enzyme cascade reaction, comprising of *Pm*LTTA, carboxylic acid reductase, alcohol dehydrogenase and glucose dehydrogenase, was constructed to prepare L-*threo*-phenylserine from cheap benzoic acid, in which alleviated inhibition of aldehydes and desirable diastereoselectivity were achieved. Under the optimized conditions, the conversion ratio of 57.1% and *de* value of 95.3% were reached. This study provides an efficient and green approach for the synthesis of chiral L-*threo*-phenylserine from industrial byproduct, and provides guidance for the development of cascade reactions influenced by the toxic intermediates and complicated kinetic/thermodynamic controls.

Keywords L-Thronine transaldolase · L-*Threo*-phenylserine · Reaction optimization · Cascade reaction · Diastereoselectivity

Introduction

Chiral β-hydroxy-α-amino acids are valuable chiral intermediates in the preparation of pharmaceuticals, agrochemicals, and bioactive products. For instance, L-*threo*-phenylserine (L-*t*-PS) can be used for the synthesis of cyclomarin A, an antiviral, antibiotic and antimalaria bioactive cyclic peptides especially against *Mycobacterium tuberculosis* [1]. L-*Threo*-3,4-dihydroxyphenylserine (Droxidopa) has been used for the treatment of Parkinson's disease [2–4]. L-*Threo*-*p*-nitrophenylserine is the essential for the synthesis of chloramphenicol [5]. L-*Threo*-*p*-methylsulfonylphenylserine is a key intermediate of thiamphenicol [6]. Therefore, efficient and stereoselective synthesis of β-hydroxy-α-amino acids is of great interests.

β-Hydroxy-α-amino acids have four diastereoisomers, due to two chiral centers at C_α and C_β positions [7]. It is usually difficult to synthesize enantiomeric pure β-hydroxy-α-amino acids. Extensive efforts have been devoted to develop asymmetric synthesis approaches, including sharpless asymmetric dihydroxylation, epoxidation, enzymatic aldol addition, electrochemical methods etc. [8–10]. Among them, enzymatic synthesis of β-hydroxy-α-amino acids catalyzed by aldolases or transaldolases is regarded as a promising approach, since two chiral centers could be constructed in a single step. In addition, biocatalytic approach has attracted increasing attentions due to its high atomic economy, easy operation and mild reaction conditions.

Several enzymes have been reported with efficacy in the synthesis of β-hydroxy-α-amino acids, including L-threonine aldolase (LTA), serine hydroxy methyltransferase (SHMT),

✉ Guochao Xu
guochaoxu@jiangnan.edu.cn

✉ Ye Ni
yni@jiangnan.edu.cn

[1] Key Laboratory of Industrial Biotechnology, Ministry of Education, School of Biotechnology, Jiangnan University, Wuxi 214122, Jiangsu, China

and L-threonine transaldolase (LTTA). LTA could catalyze the aldol reaction between aldehyde and glycine to produce β-hydroxy-α-amino acids. However, the stereoselectivity at C_β is usually poor, which hinders the application of LTA [6]. Recently, LTTA of aspartate aminotransferase (AAT) superfamily has been reported with relatively high stereoselectivity in transaldolation of L-threonine and aldehydes to produce β-hydroxy-α-amino acids [11]. However, equal amount of acetaldehyde was produced as a byproduct [12], together with substrate aldehydes, which could strongly inhibit the activity of LTTA due to their strong reactivity [13]. Moreover, Dimethyl sulfoxide (DMSO) should be added as co-solvent to elevate the solubility of substrate aldehyde, which is toxic to enzymes.

In this study, a novel L-threonine transaldolase *Pm*LTTA was identified from *Pseudomonas* sp. by genome mining. *Pm*LTTA exhibited desirable activity in the transaldolation of benzaldehyde and L-threonine to produce L-*t*-PS. However, there are two major issues to be addressed in the *Pm*LTTA catalyzed transaldolation reaction, moderate conversion ratio and variable diastereoselectivity. To eliminate the inhibitory effect of aldehydes, an alcohol dehydrogenase (ADH) was employed to convert the byproduct acetaldehyde into ethanol. In addition, a carboxylic acid reductase (CAR) was introduced to catalyzed the reduction of cheaper benzoic acid into benzaldehyde, which could be further utilized as substrate in LTTA-catalyzed reaction. Consequently, a multi-enzyme cascade reaction consisted of CAR, LTTA, ADH and glucose dehydrogenase (GDH, cofactor regeneration enzyme) was constructed for the synthesis of L-*t*-PS from benzoic acid. Influencing factors in the cascade reaction, such as pH, temperature, enzyme loading ratio of CAR and LTTA, amount of L-threonine etc., were systematically explored. Under the optimized conditions, the final conversion and *de* values reached 57.1% and 95.3%, respectively.

Materials and methods

Materials

Escherichia coli BL21(DE3) and pET28a were preserved in our laboratory and served as host strain and expression vector, respectively. Benzaldehyde, acetaldehyde, benzoic acid, sodium benzoate and D/L-*threo*-phenylserine (D/L-*t*-PS) were purchased from Sinopharm Chemical Reagent Co. Ltd. (China). Pyridoxal 5′-phosphate (PLP), *o*-phthaldialdehyde (OPA) and *N*-acetyl-cysteine (NAC) were obtained from Sigma-Aldrich (USA). L-Threonine was purchased from Macklin (China), D/L-*erythro*-phenylserine (D/L-*e*-PS) was purchased from Wako Pure Chemical Industries, Ltd. (Japan).

Bacterial genomic DNA extraction kits and coenzymes such as NADH were obtained from Shanghai Sangon Biotech Co., (China). All other chemicals and reagents of analytical grade were obtained from commercial source unless otherwise stated.

Construction of recombinant plasmids

The amino acid sequence of *Ps*LTTA from *Pseudomonas* sp. was used as a probe sequence (GenBank accession number: WP_065936857) [11] for BLASTp search in NCBI. Several genes coding for putative L-threonine transaldolase were selected for heterogeneous expression and functional analysis. These genes were synthesized by Talen-bio Scientific (Shanghai) Co., Ltd. and ligated into pET28a plasmid between the restriction sites of *Nde*I and *Xho*I. The obtained recombinant plasmid was transformed into *E. coli* BL21(DE3) and confirmed by DNA sequencing.

Protein expression and purification

The recombinant *E. coli* BL21(DE3) strains harboring target genes were inoculated in LB medium containing 50 μg mL^{-1} kanamycin, and cultivated at 37 °C and 180 rpm. When OD_{600} reached 0.6–0.8, 0.2 mM IPTG was added into the culture for expression of protein at 16 °C and 180 rpm for 16 h. Then the cells were harvested by centrifugation (8000 rpm, 5 min) at 4 °C. Cells were suspended in the binding buffer (0.5 M NaCl, 20 mM imidazole, 20 mM NaH_2PO_4–Na_2HPO_4, 5% glycerol, pH 7.4) and disrupted by ultrasonication in ice-water bath, then centrifuged at 4 °C and 8000 rpm to obtain the supernatant as crude enzyme extract. The recombinant enzyme with His-Tag was purified by Ni–NTA affinity chromatography. The samples were further concentrated, desalted, and then quickly frozen in liquid nitrogen and stored at –80 °C for further use. The protein concentration was determined by the Coomassie brilliant blue method.

Activity assay

The activity of LTTA was determined by ADH coupled method based on the changes of NADH [14]. The changes of NADH was determined using a PowerWave XS2 microplate reader (BioTek, USA) to monitor the decrease in absorbance at 340 nm ($\varepsilon = 6220\ M^{-1}\ cm^{-1}$) and 25 °C. The reaction system (180 μL) consisted of 100 mM HEPES–NaOH buffer (pH 8.0), 10 mM benzaldehyde, 50 mM L-threonine, 0.2 mM PLP, 1 mM NADH and 30 U ADH. After addition of 20 μL enzyme solution, the absorbance at 340 nm was monitored for 3 min. Negative control was performed with enzymes boiled at 100 °C for 10 min. One unit (U) of LTTA activity is defined as the amount of enzyme that catalyzes the

conversion of 1 μmol of phenylserine per min under above mentioned conditions.

The activity of ADH in the reduction of acetaldehyde into ethanol was determined according to the decrease of NADH at 340 nm. The reaction system (180 μL) consisted of 100 mM HEPES–NaOH buffer (pH8.0), 5 mM acetaldehyde and 1 mM NADH. After addition of 20 μL enzyme solution, the absorbance of each well was monitored at 340 nm for 3 min. Negative control was performed with enzyme boiled at 100 °C for 10 min. One unit (U) of ADH activity is defined as the amount of enzyme that catalyzes the conversion of 1 μmol acetaldehyde per min under above mentioned conditions.

The activity of CAR in reduction of benzoic acid into benzaldehyde was measured by the decrease of NAPDH at 340 nm. The reaction system (180 μL) consisted of 100 mM HEPES–NaOH buffer (pH 8.0), 5 mM benzoic acid, 1 mM NADPH, 4 mM ATP and 10 mM Mg^{2+}. After addition of 20 μL enzyme solution, the absorbance of each well was monitored at 340 nm for 3 min. The boiled enzyme was used as a negative control. One unit (U) of CAR activity is defined as the amount of enzyme that catalyzes the conversion of 1 μmol of benzoic acid per min under above mentioned conditions.

The activity of GDH in oxidation of glucose into gluconic acid was determined by the increase of NADH at 340 nm. The reaction system (180 μL) consisted of 100 mM HEPES–NaOH buffer (pH 8.0), 5 mM glucose and 1 mM NAD^+. After addition of 20 μL enzyme solution, the absorbance of each well was monitored at 340 nm for 3 min. Boiled enzyme was used as the negative control. One unit (U) of GDH activity is defined as the amount of enzyme that catalyzes the conversion of 1 μmol of glucose per min.

All experiments were performed in triplicate.

Determination of kinetic parameters

General protocol for the determination of the activity of *Pm*LTTA using microplate reader was as described in "Activity assay". Kinetic parameters of the purified *Pm*LTTA were determined using the general protocol except for different L-threonine concentration ranging from 0.1 mM to 200 mM was used [11]. All assay was conducted in triplicate. The values of kinetic parameters were calculated by fitting to Michaelis–Menten equation using GraphPad.

Effect of temperature, pH and metal ions on enzymatic activity

Effect of pH on the activity of *Pm*LTTA was investigated in different buffers, including MES–NaOH buffer (pH 5.5–6.5), HEPES–NaOH buffer (pH 7.0–8.0), PBS buffer (pH 6.0–8.0) and Tris–HCl buffer (pH 8.0–10.0). The initial conversion ratio and diastereoselectivity were analyzed to calculate the activity of *Pm*LTTA at different conditions.

Influence of temperature was also explored at different temperature ranging from 25 to 100 °C. Thermostability of *Pm*LTTA was investigated by incubation of purified enzyme (1 mg mL^{-1}) at 30, 40 and 50 °C, and at different time interval, samples were withdrawn to determine the residual activity. The changes of activity at different temperature were monitored until residual activities were lower than 50%.

Dependence of metal ions on the activity of *Pm*LTTA was examined by incubation of enzyme with different metal ions of a final concentration of 1 mM at 30 °C for 2 h. The activity of *Pm*LTTA without metal ion was regarded as 100%.

The relative activities of *Pm*LTTA were determined using the method as descripted in "Activity assay". All experiments were performed in triplicate.

HPLC analysis after OPA/NAC derivatization

The phenylserine products were derivatized using *o*-phthaldialdehyde/*N*-acetyl-cysteine (OPA/NAC) and subjected to HPLC analysis to calculate conversion ratio and diastereoselectivity [15]. The ratio of OPA/NAC reagent and reaction solution was 4:1 [11]. The derivatized reaction mixture was analyzed by Agilent 1260 Infinity HPLC system equipped with a Diamonsil C18 column (Dikma, 250 × 4.6 mm), using mobile phase of 50 mM KH_2PO_4 (pH 8.0)/acetonitrile (81/19) at a flow rate of 1 mL min^{-1}, column temperature of 30 °C, and detection wavelength of 338 nm:

$$de\% = \frac{[L-t-\mathrm{PS}]-[L-e-\mathrm{PS}]}{[L-t-\mathrm{PS}]+[L-e-\mathrm{PS}]} \times 100\%$$

Optimization of cascade reaction conditions for the synthesis of phenylserine

A cascade reaction including CAR, LTTA, ADH and GDH was developed for preparation of L-*t*-PS from benzoic acid (or sodium benzoate). The initial reaction system consisted of 100 mM HEPES–NaOH buffer (pH 8.0), 10 mM benzoic acid, 4 mM glucose, 4 mM ATP, 5 mM Mg^{2+}, 1 mM $NADP^+$, 25 mM L-threonine, 0.2 mM PLP, 1 mM NAD^+ and appropriate amount of *Pm*LTTA, CAR, GDH and ADH. Effects of enzyme addition ratio, temperature, pH and L-threonine amount on the cascade reaction were investigated, by varying amount of *Pm*LTTA (0.0125, 0.025, 0.05, 0.1, 0.2, 0.4, 0.6, 0.8, 1, 1.5, 2, 2.5 and 3 U mL^{-1}), HEPES–NaOH buffer of different pH values (pH 7.0, 8.0), Tris–HCl buffer of different pH (pH 8.0, 9.0, 10.0), different temperature (15, 20, 25, 30 and 35 °C), different amount of L-threonine (10, 15, 20, 25 and 50 mM).

Finally, the cascade reaction was performed under the optimal conditions. The reaction mixture, compromising 100 mM HEPES–NaOH buffer (pH 8.0), 10 mM sodium benzoate, 4 mM glucose, 10 mM ATP, 5 mM Mg^{2+}, 1 mM $NADP^+$, 25 mM L-threonine, 0.2 mM PLP, 1 mM NAD^+ and 1 U mL^{-1} *Pm*LTTA, 0.1 U mL^{-1} CAR, 1 U mL^{-1} GDH and 1 U mL^{-1} ADH, was conducted at 25 °C for 12 h.

The conversion and diastereoselectivity were calculated based on HPLC analysis after OPA/NAC derivatization as descripted above.

Results and discussion

Identification of L-threonine transaldolases

Nine putative LTTAs with 30–80% sequence similarity (Table S1) were selected from GenBank database, based on BLASTp search with *Ps*LTTA as a probe sequence [11]. All these LTTAs could be heterogeneously expressed in *E. coli* BL21(DE3) in soluble form. Then, the specific activities of these enzymes were measured and summarized in Fig. 1a. The specific activity of *Ps*LTTA was regarded as 100%. All nine putative LTTAs exhibited transaldolase activity toward benzaldehyde and L-threonine. The activities of LTTAs from *Pseudomonas* sp. (*Pm*LTTA) and *Chitiniphilus eburneus* (*Ce*LTTA) were higher than that of *Ps*LTTA. *Pm*LTTA exhibited the highest catalytic efficiency with relative activity of 166% of that of *Ps*LTTA. To further examine the potential of *Pm*LTTA in the biotransformation, the conversion ratio was monitored and compared with *Ps*LTTA (Fig. 1b). The conversion ratio of *Pm*LTTA reached 19.4% within 1.5 h, and kept constant until 12 h. The conversion ratio of *Ps*LTTA increased steadily to 17.2% at 12 h. Using the same enzyme loading, the conversion ratio of *Pm*LTTA remained higher than that of *Ps*LTTA during 12 h of reaction. All above indicated *Pm*LTTA is an efficient L-threonine transaldolase for the synthesis of chiral β-hydroxy-α-amino acids.

Enzymatic properties of *Pm*LTTA

Sequence analysis revealed that this newly identified *Pm*LTTA shares 79% sequence similarity with *Ps*LTTA. Multiple sequence alignment was performed with *Pm*LTTA and reported transaldolases from AAT superfamily, including ObiH, *De*SHMT, *Th*SHMT, *Ca*SHMT [16–18] (Table S2). According to the crystal structure of ObiH [16], the PLP-binding residues include Lys234, Arg366, His131, Tyr55, Asn268 and Asp204, which are also conserved in *Pm*LTTA and other reported AAT superfamily member (Fig. S1), indicating *Pm*LTTA might share a common evolutionary origin [19–21] and belong to the PLP fold type I superfamily [22–24]. The phylogenetic analysis [19] indicates that *Pm*LTTA has a separate evolutionary direction, although it shares a common evolutionary origin with SHMT and LTA (Fig. S2).

The recombinant *Pm*LTTA was purified using nickel affinity chromatography. A pink enzyme solution was obtained after purification (Fig. S3a), which is consistent with previously reported phenomenon [11, 16]. The pink color of the enzyme is mainly attributed to the internal aldimine formed between PLP and the Lys residue, which would form a pink internal quinonoid after deprotonation, with the maximum absorbance at 515 nm. SDS–PAGE analysis indicated that *Pm*LTTA was expressed in soluble form

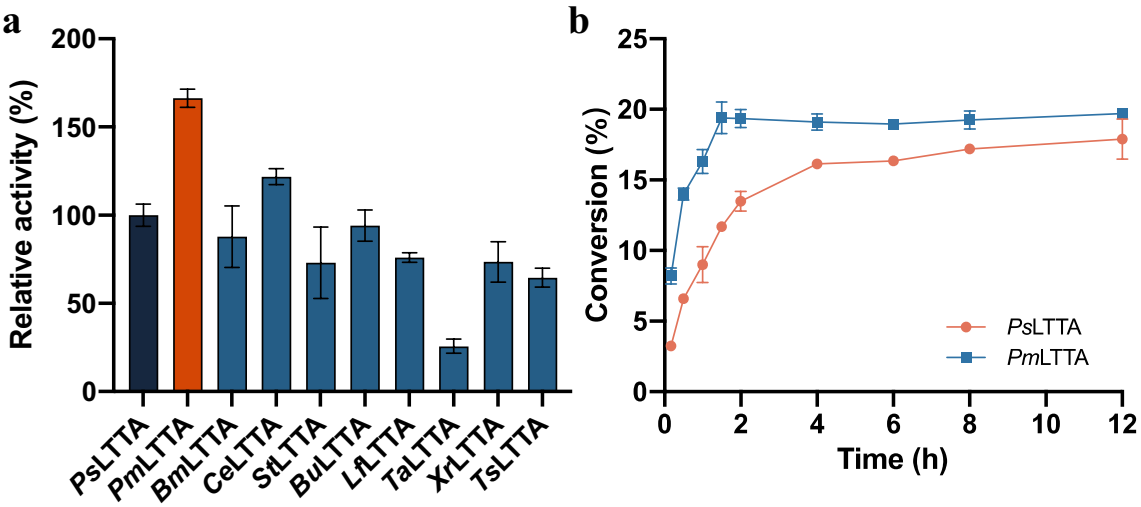

Fig. 1 **a** Relative activity of various LTTAs. **b** Time course of transaldolation reaction catalyzed by *Ps*LTTA and *Pm*LTTA. The specific activity of *Ps*LTTA was regarded as 100%

and migrated at about 49 kDa (Fig. S3b), agreed with the theoretical molecular weight of about 49 kDa. The specific activity of purified *Pm*LTTA was determined to be 5.48 U mg^{-1}, which was 16.6-fold of crude extract (0.33 U mg^{-1}). The K_M and k_{cat} values of *Pm*LTTA toward L-threonine were 5.62 ± 0.49 mM and 3.0 ± 0.06 s^{-1} mM^{-1}, respectively.

Effect of temperature on the purified *Pm*LTTA was investigated as shown in Fig. 2a, b. The activity of *Pm*LTTA increased with the temperature from 25 °C to 70 °C (Fig. 2a). At temperatures higher than 70 °C, the activity decreased sharply, indicating the optimal temperature of *Pm*LTTA was 70 °C. The half-life of *Pm*LTTA was determined by incubation purified *Pm*LTTA at different temperature. The half-lives of *Pm*LTTA at 30 °C, 40 °C, and 50 °C were about 26 h, 7 h, and 100 min, respectively (Fig. 2b). The results suggest that *Pm*LTTA is a thermostable and promising biocatalyst for scale-up application.

Influence of pH and buffer system on the activity of *Pm*LTTA was also explored. As shown in Fig. 2c, *Pm*LTTA displayed the highest activity at pH 8.0 in PBS buffer. Besides, biocompatible buffers, such as HEPES–NaOH and MES–NaOH, were also examined. At the same pH value, *Pm*LTTA exhibited higher activities in MES–NaOH and HEPES–NaOH systems than that of PBS buffer. For example, the activity in PBS buffer (pH 8.0) was only 57% of that in HEPES–NaOH buffer (pH 8.0). As a result, HEPES–NaOH (pH 8.0, 100 mM) was selected for further experiments.

Dependence of *Pm*LTTA on metal ions was also evaluated. As shown in Fig. 2d, control experiment without metal ions was regarded as 100%. Only Mg^{2+} could slightly promote the transaldolase activity of *Pm*LTTA, with relative activity of 121%. The activity of *Pm*LTTA was barely influenced by Ca^{2+}, Mn^{2+}, Ni^{2+}, Ba^{2+}. Obvious inhibitory effect was found with Co^{2+}, Cu^{2+}, $Fe^{2+}$and Zn^{2+}. All above indicated that *Pm*LTTA is not a metal enzyme.

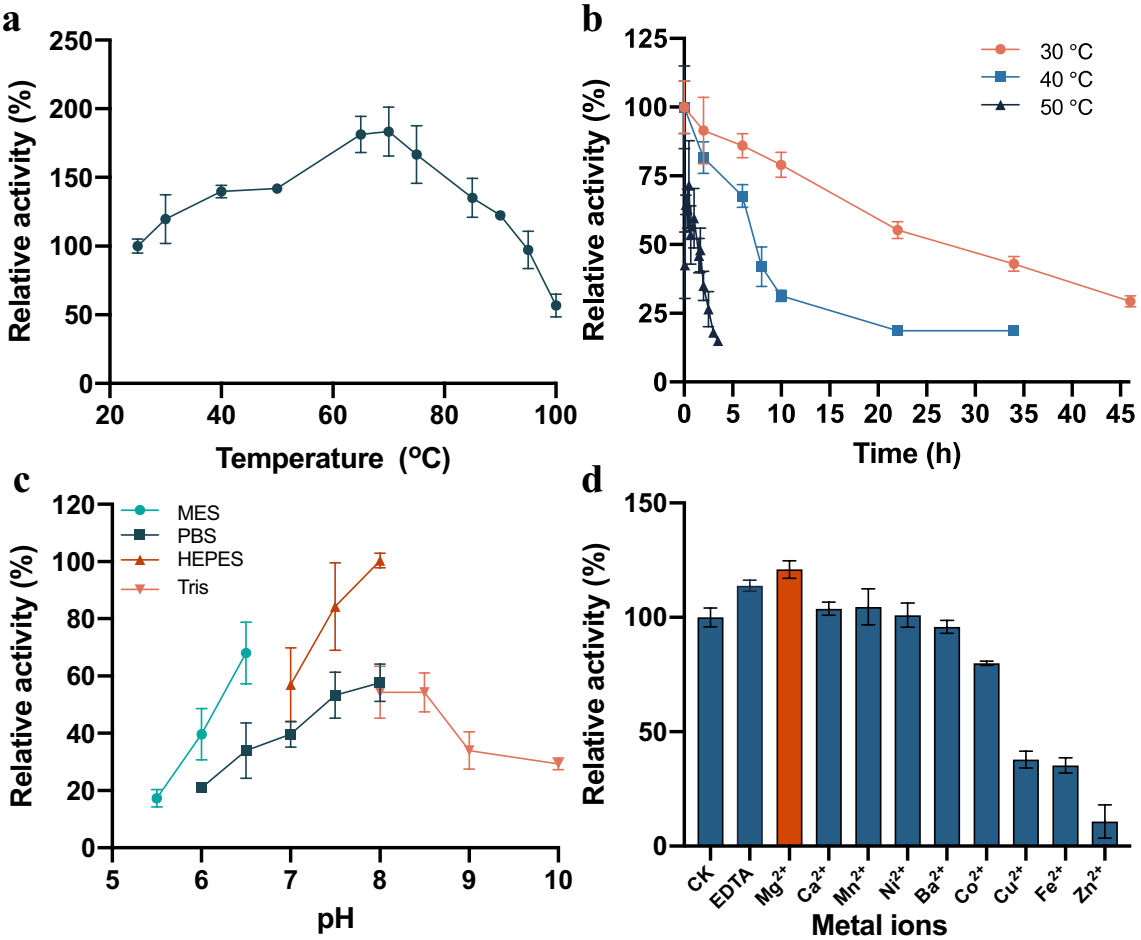

Fig. 2 Enzymatic properties of *Pm*LTTA. **a** Temperature profile of *Pm*LTTA. **b** Thermostability of *Pm*LTTA 30 °C, 40 °C and 50 °C. **c** pH profile of *Pm*LTTA. **d** Metal ions dependence of *Pm*LTTA

Identification of bottlenecks in enzymatic transaldolation reaction

To establish an efficient biocatalytic process for the synthesis of chiral β-hydroxy-α-amino acids, effects of the amount of *Pm*LTTA and reaction time on the conversion ratio and diastereoselectivity were evaluated using benzaldehyde and L-threonine as substrates. As shown in Fig. 3a, the increase of enzyme loading led to increased conversion ratio, however, decreased diastereoselectivity, which was also observed in previous reports [11]. At *Pm*LTTA amounts of 0.1 and 0.2 U mL^{-1}, the *de* value of L-*t*-PS was about 88.2%, then the *de* value decreased to 68.6% with an increased enzyme loading to 1 U mL^{-1}. The results indicate that lower enzyme loading is favorable to the formation of L-*threo* isomer. Although the diastereoselectivity values at 0.1 and 0.2 U mL^{-1} *Pm*LTTA were similar, the conversion ratio was 5% higher at 0.2 U mL^{-1}, suggesting that the optimal *Pm*LTTA amount is 0.2 U mL^{-1}.

Furthermore, the changes of conversion ratios and diastereoselectivities under 0.2 U mL^{-1} *Pm*LTTA were monitored (Fig. 3b). The conversion ratios increased from 15.2% at 1 h to 24.9% at 6 h. Further elongated reaction time did not result in further increased conversion ratio. The low conversion ratios might be attributed to the toxicity of benzaldehyde and acetaldehyde. Moreover, the diastereoselectivity value decreased from 92.5% at 1 h to 84.6% at 6 h. This phenomenon is similar to the influence of increased enzyme amount, which has also been observed in aldolases catalyzed reaction [25]. The results indicate that the transaldolation reaction might also be regulated by both kinetic control and thermodynamic control. At the initial stage, the reaction is mainly controlled by kinetic control with better diastereoselectivity, and as the reaction time proceeds, the amount of thermodynamic products increased, resulting in progressively decreased diastereoselectivity.

It was noted that the conversion ratio was less than 25% and the diastereoselectivity decreased during the reaction, representing two bottlenecks for the application of *Pm*LTTA in the synthesis of chiral β-hydroxy-α-amino acids. To solve the issues, we envisioned to introduce CAR and ADH to decrease the adverse impact of benzaldehyde and acetaldehyde on the conversion ratio and diastereoselectivity.

Construction and optimization of the cascade reaction

Introduce of alcohol dehydrogeanse

To eliminate the influence of acetaldehyde on the *de* value and conversion ratio, alcohol dehydrogenase from *Saccharomyces cerevisiae* (*Sc*ADH) was cloned and introduced in the *Pm*LTTA catalyzed reaction system, which could convert the acetaldehyde generated from L-threonine into ethanol (Fig. 4a). As above mentioned, accumulation of acetaldehyde would lead to the decrease of conversion ratio. Moreover, removal of acetaldehyde, one of the products, could shift the equilibrium toward the generation of β-hydroxy-α-amino acid and overcome the thermodynamic limitation [25, 26]. Hence, the *de* values might also become stable during the reaction. Considering *Sc*ADH is NADH-dependent, glucose dehydrogenase from *Bacillus megaterium* (*Bm*GDH) was employed for regeneration of NADH. As shown in Fig. 4b, c, the conversion ratio of *Pm*LTTA coupled with *Sc*ADH were higher than *Pm*LTTA during the reaction. At the end of 6 h, the conversion ratio of *Pm*LTTA/*Sc*ADH-coupled reaction

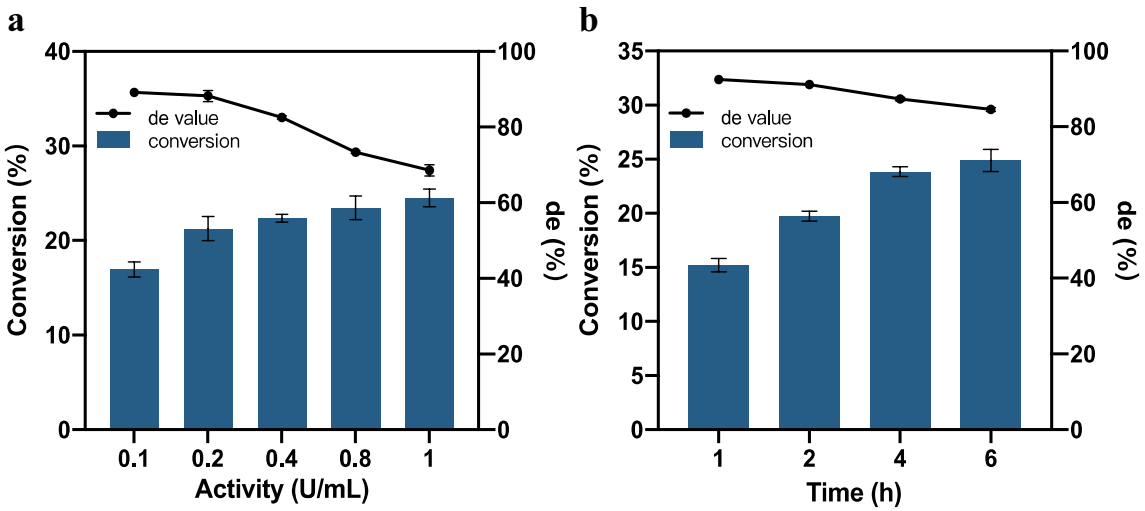

Fig. 3 **a** Effect of enzyme loading on the conversion ratio and diastereoselectivity of *Pm*LTTA. **b** Time course of *Pm*LTTA catalyzed transaldolation reaction of L-threonine and benzaldehyde

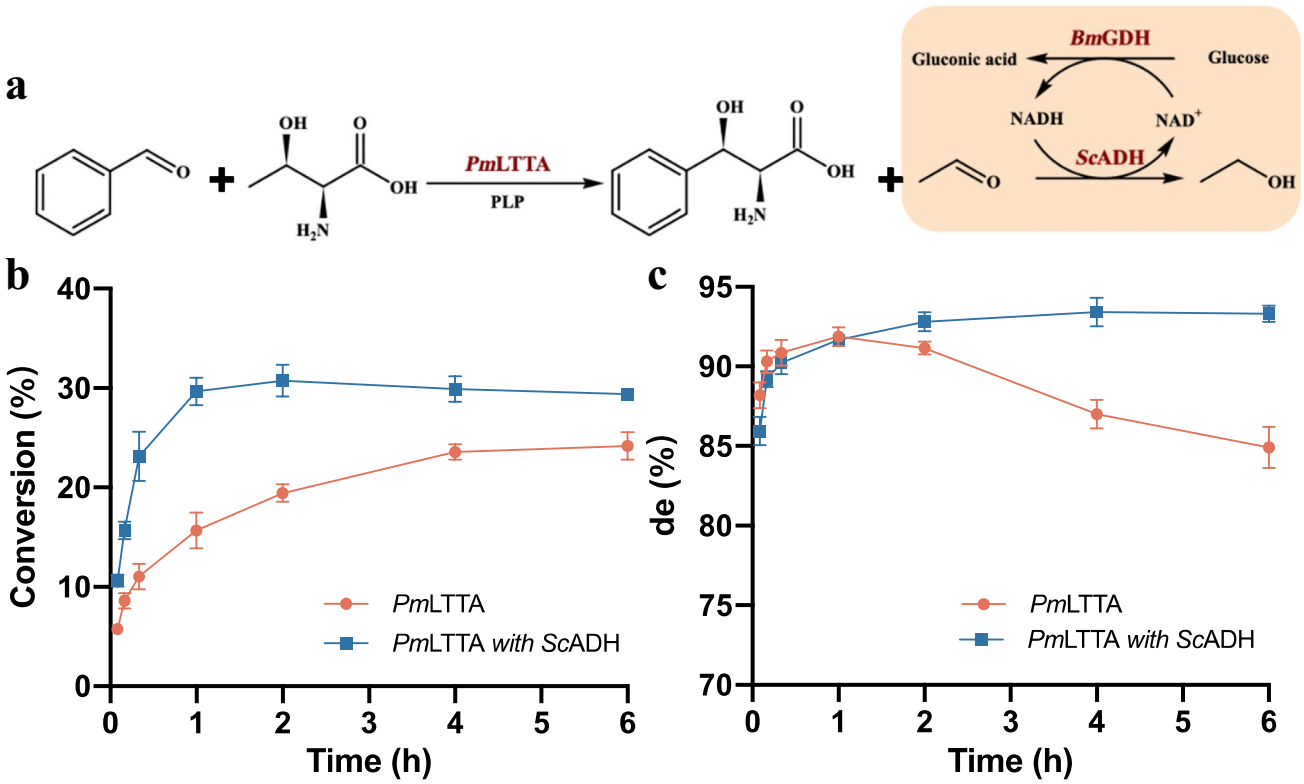

Fig. 4 Asymmetric synthesis of L-*t*-PS by *Pm*LTTA coupled with *Sc*ADH and *Bm*GDH. **a** Scheme of the cascade reaction. **b** Comparison of the conversion ratios of cascade reaction coupled with/without *Sc*ADH. **c** Comparison of the *de* values of cascade reaction coupled with/without *Sc*ADH. Reaction conditions: 1 mL reaction mixture containing 10 mM benzaldehyde, 4 mM glucose, 1 mM Mg^{2+}, 25 mM L-threonine, 0.2 mM PLP, 1 mM NAD^+ and 0.2 U mL^{-1} *Pm*LTTA, 1 U mL^{-1} *Sc*ADH, 1 U mL^{-1} *Bm*GDH in HEPES–NaOH buffer (100 mM HEPES–NaOH, pH 8.0) at 30 °C

was 29.4%, which was 5% higher than that of *Pm*LTTA. Most importantly, the *de* values did not decrease with the prolongation of reaction time, and remained stable of 93.4% at 6 h, while the *de* values decreased to 84.9% in reaction without *Sc*ADH. Therefore, the introduce of ADH could alleviate the adverse effects of acetaldehyde and significantly increase the conversion ratios and diastereoselectivity.

Introduce of carboxylic acid reductase

To further reduce the inhibitory effect of benzaldehyde on *Pm*LTTA, CAR was introduced. CAR could catalyze the reduction of benzoic acid into benzaldehyde (Fig. 5a), which could further be utilized by *Pm*LTTA. Thus, the concentration of benzaldehyde in the reaction system could be maintained at a relative lower level. Moreover, benzoic acid is usually regarded as a cheap industrial byproduct, which is also of environmental interest. To achieve the efficient conversion of benzoic acid into benzaldehyde, several CARs, including *Ma*CAR [27], *Ni*CAR [28] and mutant $NiCAR^{Q283P}$ [29] with higher activities, *Anc*CAR-A and *Anc*CAR-PF [30] with better thermal stability were evaluated for cascade reaction. First, the specific activities of pure enzyme toward benzoic acid were determined, as shown in Fig. 5b. The specific activity of $NiCAR^{Q283P}$ was 101.6 U g^{-1}, ranking the highest, while the specific activity of *Anc*CAR-PF was the lowest. The specific activity of *Anc*CAR-A was 25.1 U g^{-1}. Furthermore, the potential of these CARs in the cascade reaction were evaluated. The conversion ratios and *de* values of the CARs participated cascade reaction were monitored, as illustrated in Fig. 5c, d. Unlike the reaction without CARs, the conversion ratios increased progressively until 12 h. In addition, the conversion ratios of *Anc*CAR-A and *Anc*CAR-PF with better thermal stability were significantly higher than that of other enzymes. The conversion ratio of *Anc*CAR-A was about 13.5% higher than that obtained by *Ni*CAR participated reaction, although the specific activity of *Anc*CAR-A was much lower than that of *Ni*CAR. Interestingly, the *de* values obtained by *Anc*CAR-A and *Anc*CAR-PF participated reactions also ranked the highest, which were 96.5% and 95.3%, respectively, at 12 h. All above proved that *Anc*CAR-A and *Anc*CAR-PF with higher thermal stability are more suitable for cascade reactions, especially for reactions require longer duration. As a result, *Anc*CAR-A, displaying the highest conversion ratio (25.8%) and *de*

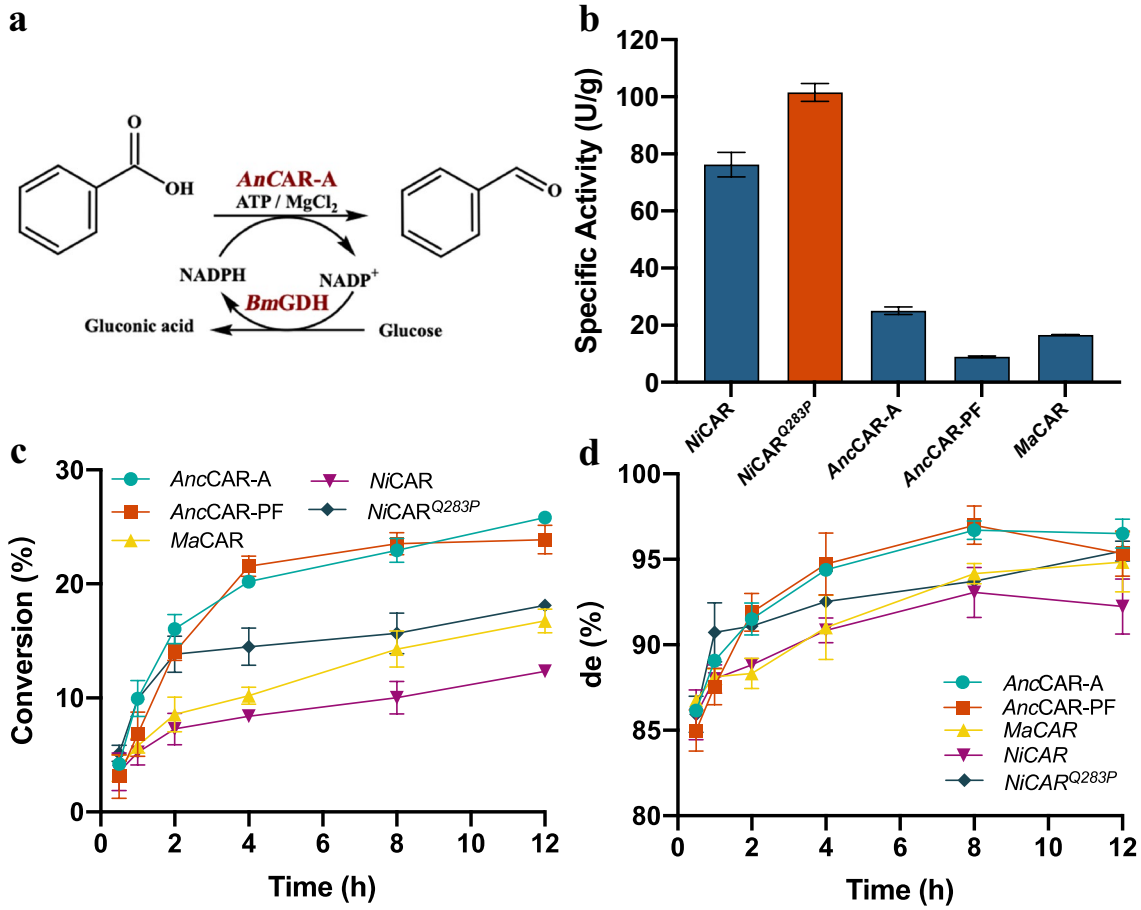

Fig. 5 Effect of CAR on the conversion ratio and diastereoselectivity of *Pm*LTTA. **a** Scheme of the synthesis of benzaldehyde from benzoic acid by *Anc*CAR-A coupled with *Bm*GDH. **b** Specific activities of CARs toward benzoic acid. **c** Effect of CARs on the conversion ratios of cascade reaction. **d** Effect of CARs on the *de* value of cascade reaction. Reaction conditions: 1 mL reaction mixture containing 10 mM benzoic acid, 4 mM glucose, 10 mM ATP, 5 mM Mg^{2+}, 1 mM $NADP^+$ and 0.1 U mL^{-1} *Anc*CAR-A, 1 U mL^{-1} *Bm*GDH in HEPES–NaOH buffer (100 mM HEPES–NaOH, pH 8.0) at 30 °C

value (96.5%) in cascade reaction, was selected for further experiment.

Optimization of multi-enzyme cascade reaction

A CAR–LTTA cascade reaction was developed for the synthesis of L-*t*-PS from benzoic acid (Fig. 6a). To further increase the conversion ratio and diastereoselectivity, factors influencing the cascade reaction, such as pH, temperature, enzyme loading ratio of CAR and LTTA, L-threonine and ATP, were systematically explored.

Aqueous soluble sodium benzoate was used instead of benzoic acid to avoid the addition of co-solvents, such as DMSO, which could be toxic to enzymes. The conversion ratio and diastereoselectivity of the benzoic acid and sodium benzoate were compared and shown in Fig. S4a. The conversion ratio of sodium benzoate was 17.3%, which was higher than 13.8% of benzoic acid.

Influence of the pH values of HEPES buffer on the cascade reaction was also investigated. As shown in Fig. 6b, as the pH increased from 7.0 to 8.0, the conversion ratios increased from 12.6 to 22.1%. Furthermore, the conversion ratio was not influenced at pHs higher than 8.0. It should be noted that the pH of reaction system has little impact on diastereoselectivity, with *de* values stabilized at around 94.5% from pH 7.0 to 10.0. Therefore, pH 8.0 of HEPES buffer was chosen for this newly developed cascade reaction. Considering CAR is ATP-dependent, the influence of ATP concentrations (4 mM, 10 mM, 20 mM) on the cascade reaction was also evaluated. As shown in Fig. S4b, the highest conversion ratio (36.5%) and *de* value (96.9%) were observed in 10 mM ATP. Either lower or higher ATP concentrations were not favorable for this cascade reaction. The results show that the lower ATP concentration could reduce the synthesis of benzaldehyde catalyzed by CAR, and thus affect the conversion ratio of the cascade reaction. While higher ATP concentration could lead to the accumulation

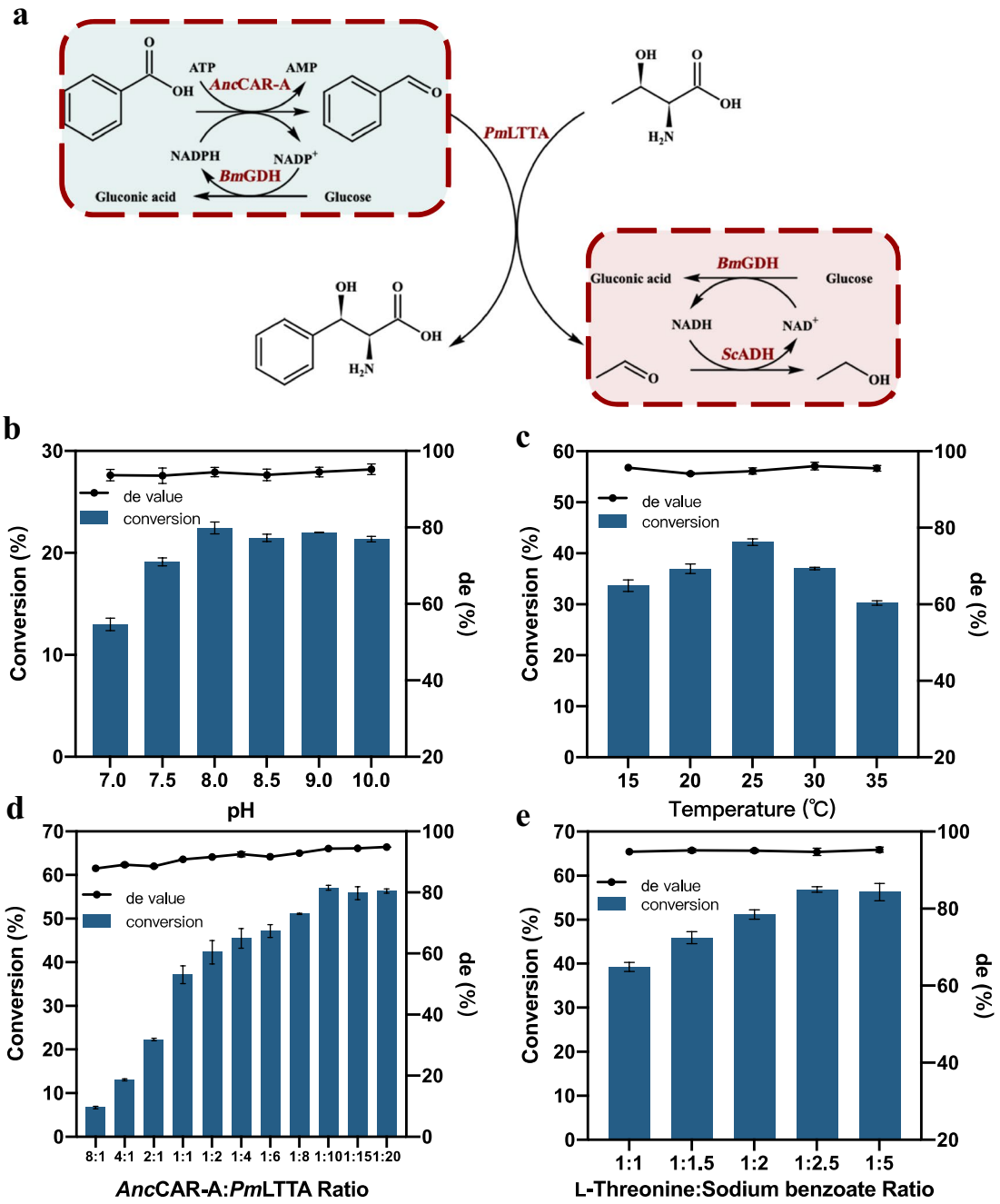

Fig. 6 Development of cascade reaction consisted of *Pm*LTTA, *Anc*CAR-A, *Sc*ADH and *Bm*GDH for efficient asymmetric synthesis of L-*t*-PS. **a** Scheme of the cascade reaction. **b** Effect of pH on the cascade reaction. **c** Effect of temperature on the cascade reaction. **d** Effect of enzyme loading ratios. **e** Effect of L-threonine addition amount. Reaction conditions: 1 mL reaction mixture containing 10 mM sodium benzoate, 4 mM glucose, 10 mM ATP, 5 mM Mg^{2+}, 1 mM $NADP^+$, 25 mM L-threonine, 0.2 mM PLP, 1 mM NAD^+ and 1 U mL^{-1} *Pm*LTTA, 0.1 U mL^{-1} *Anc*CAR-A, 1 U mL^{-1} *Sc*ADH, 1 U mL^{-1} *Bm*GDH

of benzaldehyde and, therefore, inhibit the reaction rate of cascade system.

The cascade reaction was evaluated at 15 °C, 20 °C, 25 °C, 30 °C and 35 °C. As illustrated in Fig. 6c, the conversion ratios increased as the temperature increased from 15 °C to 25 °C, and the highest conversion ratio of 42.2% was observed at 25 °C. At temperatures higher than 25 °C, the conversion ratios decreased, with only 30.2%

at 35 °C. For this cascade reaction, the thermostability of CAR and LTTA plays an important role. Higher thermostability of CAR could be beneficial to higher conversion ratio. Moreover, the around 94% *de* was determined under different temperatures. Therefore, 25 °C was chosen as the optimal temperature of cascade reaction.

The enzyme loading ratios of *Anc*CAR-A to *Pm*LTTA, ranging from 8:1 to 1:20, were investigated. As shown in Fig. 6d, with higher loading of *Pm*LTTA such as ratios of 8:1 to 1:1, the conversion ratios significantly increased from 6.7 to 37.2%, indicating that the amount of *Pm*LTTA is critical for the cascade reaction. Then, elevated amount of *Pm*LTTA from 1:1 to 1:20 was attempted. Further increased conversion ratio was observed, and the highest conversion ratio of 57.1% was achieved at ratio of 1:10. At higher ratios of 1:15 and 1:20, the conversion ratios remained similar as that of 1:10. Therefore, higher amounts of *Pm*LTTA resulted in higher conversion ratios by converting of benzaldehyde into L-*t*-PS and reducing the toxicity toward enzymes in the cascade system. Variation of the enzyme loading ratio could also influence the *de* value of L-*t*-PS. The *de* values increased with the increased ratios of *Anc*CAR-A to *Pm*LTTA. At ratio of 8:1, the *de* value was 87.9%, while at ratio of 1:10, the *de* value was as high as 94.4%. Further increased the amount of *Pm*LTTA to 1:15 and 1:20 could not improve the diastereoselectivity. Hence, the enzyme loading ratio of CAR and *Pm*LTTA was determined to be 1:10 in the cascade reaction.

L-Threonine serves as the donor of glycine. Usually, glycine should be added in excess [6, 25, 31], which could drive the reaction equilibrium toward the generation of product. Different equivalents of L-threonine toward sodium benzoate were attempted in the cascade reaction. As shown in Fig. 6e, the conversion ratios increased as the increase of L-threonine equivalent from 1:1 to 1:2.5, with the highest conversion ratio of 57.1% obtained at 1:25. Further increased amount of L-threonine to 1:5 did not result in higher conversion ratio. In addition, the increase of L-threonine equivalent hardly affect the diastereselectivity. Hence, L-threonine equivalent of 1:2.5 was regarded as the optimum amount for the cascade reaction.

An efficient multi-enzyme cascade reaction has been successfully developed with significantly increased conversion ratio and stable diastereoselectivity. Under the optimized conditions, including 10 mM ATP, pH 8.0 of HEPES buffer, temperature of 25 °C, the ratio of CAR and LTTA of 1:10, L-threonine equivalent of 1:2.5, the conversion ratio of 57.1% was achieved, 1.28-fold higher than 25% of the initial reaction by *Pm*LTTA, and a stable *de* value of 95.3% was obtained (Fig. S5).

Conclusions

A novel L-threonine transaldolase *Pm*LTTA was identified from *Pseudomonas* sp. through genome mining. Characterization of *Pm*LTTA revealed that the specific activity of *Pm*LTTA was 5.48 U mg^{-1}, and the optimum pH and temperature were 8.0 and 70 °C. A multi-enzyme cascade system, consisted of *Pm*LTTA, *Anc*CAR-A, *Sc*ADH and *Bm*GDH, was successfully developed for the synthesis of chiral β-hydroxy-α-amino acids, aiming at reducing the inhibitory effect of aldehydes and improving the diastereoselectivity. Under the optimized conditions, L-*t*-PS was obtained at 57.1% conversion and 95.3% *de*, much higher than those of the initial reaction using *Pm*LTTA. Toxicity of benzaldehyde and acetaldehyde was alleviated and the distereoselectivity was stabilized in this newly designed cascade system. This study provides an efficient cascade reaction system for the synthesis of valuable chiral β-hydroxy-α-amino acids from industrial byproduct, and provides guidance for optimization of cascade reactions influenced by toxicity of aldehydes and complicated kinetic and thermodynamic controls.

Supplementary Information The online version contains supplementary material available at https://doi.org/10.1007/s43393-022-00102-x.

Acknowledgements We are grateful to the National Key Research and Development Program (2021YFC2102700), the National Natural Science Foundation of China (22077054, 22078127), the National First-Class Discipline Program of Light Industry Technology and Engineering (LITE2018-07), and Program of Introducing Talents of Discipline to Universities (111-2-06) for the financial support of this research.

Declarations

Conflict of interest The authors declare that they have no known competing financial interests or personal relationships that could have appeared to influence the work reported in this paper.

References

1. Barbie P, Kazmaier U. Total synthesis of cyclomarin A, a marine cycloheptapeptide with anti-tuberculosis and anti-malaria activity. Org Lett. 2016;18(2):204–7. https://doi.org/10.1021/acs.orglett.5b03292.
2. Gwon HJ, Baik SH. Diastereoselective synthesis of L: -*threo*-3,4-dihydroxyphenylserine by low-specific L: -threonine aldolase mutants. Biotechnol Lett. 2010;32(1):143–9. https://doi.org/10.1007/s10529-009-0125-z.
3. Zhao W, Yang B, Zha R, Zhang Z, Tang S, Pan Y, Qi N, Zhu L, Wang B. A recombinant L-threonine aldolase with high diastereoselectivity in the synthesis of L-*threo*-dihydroxyphenylserine. Biochem Eng J. 2020. https://doi.org/10.1016/j.bej.2020.107852.
4. Lamotte G, Holmes C, Sullivan P, Goldstein DS. Substantial renal conversion of L-*threo*-3,4-dihydroxyphenylserine (droxidopa) to norepinephrine in patients with neurogenic orthostatic

hypotension. Clin Auton Res. 2019;29(1):113–7. https://doi.org/10.1007/s10286-018-0564-5.
5. Zhao GH, Li H, Liu W, Zhang WG, Zhang F, Liu Q, Jiao QC. Preparation of optically active beta-hydroxy-alpha-amino acid by immobilized *Escherichia coli* cells with serine hydroxymethyl transferase activity. Amino Acids. 2011;40(1):215–20. https://doi.org/10.1007/s00726-010-0637-9.
6. Chen Q, Chen X, Feng J, Wu Q, Zhu D, Ma Y. Improving and inverting Cβ-stereoselectivity of threonine aldolase via substrate-binding-guided mutagenesis and a stepwise visual screening. ACS Catal. 2019;9(5):4462–9. https://doi.org/10.1021/acscatal.9b00859.
7. Ashford PA, Bew SP. Recent advances in the synthesis of new glycopeptide antibiotics. Chem Soc Rev. 2012;41(3):957–78. https://doi.org/10.1039/c1cs15125h.
8. Masruri WAC, McLeod MD. Osmium-catalyzed vicinal oxyamination of alkenes by *N*-(4-toluenesulfonyloxy)carbamates. J Org Chem. 2012;77(19):8480–91. https://doi.org/10.1021/jo301372y.
9. Katsuki T, Sharpless KB. The first practical method for asymmetric epoxidation. J Am Chem Soc. 1980;102(18):5974–6. https://doi.org/10.1021/ja00538a077.
10. Levitskiy OA, Grishin YK, Magdesieva TV. Stereoselective electrosynthesis of β-hydroxy-α-amino acids in the form of Ni^{II}-schiff-base complexes. Eur J Org Chem. 2019;2019(20):3174–82. https://doi.org/10.1002/ejoc.201900466.
11. Xu L, Wang L-C, Xu X-Q, Lin J. Characteristics of l-threonine transaldolase for asymmetric synthesis of β-hydroxy-α-amino acids. Catal Sci Technol. 2019;9(21):5943–52. https://doi.org/10.1039/c9cy01608b.
12. Xu L, Wang LC, Su BM, Xu XQ, Lin J. Multi-enzyme cascade for improving beta-hydroxy-alpha-amino acids production by engineering L-threonine transaldolase and combining acetaldehyde elimination system. Bioresour Technol. 2020;310: 123439. https://doi.org/10.1016/j.biortech.2020.123439.
13. Česnik M, Sudar M, Roldan R, Hernandez K, Parella T, Clapés P, Charnock S, Vasić-Rački Đ, Findrik Blažević Z. Model-based optimization of the enzymatic aldol addition of propanal to formaldehyde: a first step towards enzymatic synthesis of 3-hydroxybutyric acid. Chem Eng Res Des. 2019;150:140–52. https://doi.org/10.1016/j.cherd.2019.06.025.
14. Xu G, Dai W, Wang Y, Zhang L, Sun Z, Zhou J, Ni Y. Molecular switch manipulating Prelog priority of an alcohol dehydrogenase toward bulky-bulky ketones. Mol Catal. 2020. https://doi.org/10.1016/j.mcat.2019.110741.
15. Gong L, Xiu Y, Dong J, Han R, Xu G, Ni Y. Sustainable one-pot chemo-enzymatic synthesis of chiral furan amino acid from biomass via magnetic solid acid and threonine aldolase. Bioresour Technol. 2021;337: 125344. https://doi.org/10.1016/j.biortech.2021.125344.
16. Kumar P, Meza A, Ellis JM, Carlson GA, Bingman CA, Buller AR. L-Threonine transaldolase activity is enabled by a persistent catalytic intermediate. ACS Chem Biol. 2021;16(1):86–95. https://doi.org/10.1021/acschembio.0c00753.
17. Dombrowski N, Seitz KW, Teske AP, Baker BJ. Genomic insights into potential interdependencies in microbial hydrocarbon and nutrient cycling in hydrothermal sediments. Microbiome. 2017;5(1):106–106. https://doi.org/10.1186/s40168-017-0322-2.
18. Zhou Z, Liu Y, Xu W, Pan J, Luo Z-H, Li M. Genome- and community-level interaction insights into carbon utilization and element cycling functions of hydrothermarchaeota in hydrothermal sediment. mSystems. 2020;5(1):e00795-e1719. https://doi.org/10.1128/mSystems.00795-19.
19. Scott TA, Heine D, Qin Z, Wilkinson B. An L-threonine transaldolase is required for L-*threo*-beta-hydroxy-alpha-amino acid assembly during obafluorin biosynthesis. Nat Commun. 2017;8:15935. https://doi.org/10.1038/ncomms15935.
20. Wang S, Deng H. Peculiarities of promiscuous L-threonine transaldolases for enantioselective synthesis of beta-hydroxy-alpha-amino acids. Appl Microbiol Biotechnol. 2021;105(9):3507–20. https://doi.org/10.1007/s00253-021-11288-w.
21. Wu L, Tong MH, Raab A, Fang Q, Wang S, Kyeremeh K, Yu Y, Deng H. An unusual metal-bound 4-fluorothreonine transaldolase from *Streptomyces* sp. MA37 catalyses promiscuous transaldol reactions. Appl Microbiol Biotechnol. 2020;104(9):3885–96. https://doi.org/10.1007/s00253-020-10497-z.
22. Fesko K, Suplatov D, Švedas V. Bioinformatic analysis of the fold type I PLP-dependent enzymes reveals determinants of reaction specificity in L-threonine aldolase from *Aeromonas jandaei*. FEBS Open Bio. 2018. https://doi.org/10.1002/2211-5463.12441.
23. Steffen-Munsberg F, Vickers C, Kohls H, Land H, Mallin H, Nobili A, Skalden L, van den Bergh T, Joosten HJ, Berglund P, Höhne M, Bornscheuer UT. Bioinformatic analysis of a PLP-dependent enzyme superfamily suitable for biocatalytic applications. Biotechnol Adv. 2015;33(5):566–604. https://doi.org/10.1016/j.biotechadv.2014.12.012.
24. Eliot AC, Kirsch JF. Pyridoxal phosphate enzymes: mechanistic, structural, and evolutionary considerations. Annu Rev Biochem. 2004;73:383–415. https://doi.org/10.1146/annurev.biochem.73.011303.074021.
25. Fesko K, Reisinger C, Steinreiber J, Weber H, Schürmann M, Griengl H. Four types of threonine aldolases: similarities and differences in kinetics/thermodynamics. J Mol Catal B. 2008;52–53:19–26. https://doi.org/10.1016/j.molcatb.2007.10.010.
26. Steinreiber J, Schurmann M, Wolberg M, van Assema F, Reisinger C, Fesko K, Mink D, Griengl H. Overcoming thermodynamic and kinetic limitations of aldolase-catalyzed reactions by applying multienzymatic dynamic kinetic asymmetric transformations. Angew Chem Int Ed Engl. 2007;46(10):1624–6. https://doi.org/10.1002/anie.200604142.
27. Park J, Lee H-S, Oh J, Joo JC, Yeon YJ. A highly active carboxylic acid reductase from *Mycobacterium abscessus* for biocatalytic reduction of vanillic acid to vanillin. Biochem Eng J. 2020;161:107683. https://doi.org/10.1016/j.bej.2020.107683.
28. He A, Li T, Daniels L, Fotheringham I, Rosazza JP. *Nocardia* sp. carboxylic acid reductase: cloning, expression, and characterization of a new aldehyde oxidoreductase family. Appl Environ Microbiol. 2004;70(3):1874–81. https://doi.org/10.1128/aem.70.3.1874-1881.2004.
29. Schwendenwein D, Ressmann AK, Doerr M, Höhne M, Bornscheuer UT, Mihovilovic MD, Rudroff F, Winkler M. Random mutagenesis-driven improvement of carboxylate reductase activity using an amino benzamidoxime-mediated High-throughput assay. Adv Synth Catal. 2019. https://doi.org/10.1002/adsc.201900155.
30. Thomas A, Cutlan R, Finnigan W, van der Giezen M, Harmer N. Highly thermostable carboxylic acid reductases generated by ancestral sequence reconstruction. Commun Biol. 2019;2:429. https://doi.org/10.1038/s42003-019-0677-y.
31. Steinreiber J, Fesko K, Reisinger C, Schürmann M, van Assema F, Wolberg M, Mink D, Griengl H. Threonine aldolases—an emerging tool for organic synthesis. Tetrahedron. 2007;63(4):918–26. https://doi.org/10.1016/j.tet.2006.11.035.